RSC Advances

ROYAL SOCIETY
OF CHEMISTRY

www.rsc.org/advances

Size Dependence of the Structural, Electronic, and Optical Properties of (CdSe)$_n$, n=6-60, Nanocrystals

Michael M. Sigalas[1], Emmanuel N. Koukaras[2,3], and Aristides D. Zdetsis[2*]

[1]Department of Materials Science, University of Patras, Patras 26500 GR, Greece

[2]Molecular Engineering Laboratory, Department of Physics, University of Patras, Patras 26500 GR, Greece

[3]Foundation for Research and Technology Hellas, Institute of Chemical Engineering Sciences (FORTH/ICE-HT), Stadiou Street, Platani, Patras GR-26504, Greece

ABSTRACT

In an attempt to reconcile conflicting results in the literature and to uncover general trends in terms of size of (CdSe)$_n$ nanocrystals, we have systematically studied, within the framework of ground state and time dependent Density Functional Theory (DFT), the electronic, optical, cohesive, and vibrational properties of representative (CdSe)$_n$ nanocrystals of various sizes (n=4–60) as a function of size, applying fully relaxed and systematically generated geometries. Although we have found good agreement with particular high-level calculations and selected experimental results, our calculations revealed large deviations, especially for small nanoparticles, from alternative theoretical and experimental data. We have rationalized these discrepancies by showing that the choice of the theoretical method or of the DFT functional could have a strong impact on the value of the calculated energy and optical gaps; and that the accuracy of the experimental results could be hindered by uncertainties in determining the

nanoparticle's "diameter" and by the presence of passivating ligands. We illustrate that the relative insensitivity of the gap to the presence of particular organic ligands, such TOPO and OPMe$_3$, is largely related to the weakness of their interaction and the different spatial localization of the frontier orbitals.

*Corresponding author: zdetsis@upatras.gr

1. Introduction

Quantum dots (QD) have attracted a lot of interest because of their possible applications in light emitted diodes, in medical imaging, and solar cells. In particular, quantum dot sensitized solar cells (QDSSC) have been studied as a possible lower cost replacement of the widely used silicon based solar cells. [1] Comparing QDSSC with another low cost alternative, the dye sensitized solar cells (DSSC), the QDSSC's are more stable and their spectrum can be suitably tailored by changing the size of the QD. Experimentally, small thiol-stabilized crystalline CdSe nanoparticles, mainly of zinc-blende phase, with sizes in the range of $1.4 - 3.2$ nm were fabricated long time ago [2]. It was found that the measured first electronic transition appears at about 3eV for nanoparticles with diameter close to 1.5nm; whereas for diameters about 2.7nm the first allowed electronic transition (the optical gap) was reduced to less than 2.5eV [2] for diameters of about 2.7nm. [2] In another more recent experiment, [3] it was demonstrated that $(CdSe)_n$ nanoparticles, which are not "nanocrystals" or fragments of nanocrystals, were extremely stable for some particular values of n, such as 33 and 34. [3]. It was shown both theoretically and experimentally (X-ray analysis) that the structures of these "magic" clusters were puckered $(CdSe)_{28}$ cages that encompass either $(CdSe)_6$ or $(CdSe)_5$ subunits, [3]. Such "non-crystalline" stuffed fullerene type of structures, are not particularly studied here systematically, but they can be used as reference structures, especially in comparison to some early theoretical studies from the late 90s. In one of these early studies a tight binding model was used for the study of the effect of organic ligands in the surface reconstruction of CdSe nanoparticles. [4] In another early density functional theory (DFT) study examining $(CdSe)_n$ nanoparticles, with $n = 17, 26, 38$, time dependent DFT (TDDFT) was used in the local density approximation (LDA) quite successfully, yielding an optical gap, in fairly close agreement with

experiment [5]. However, in that study, in which the structure of the clusters was preconditioned to satisfy known experimental data, the assumption of the absorption edge as the energy threshold below which the absorption is 2% of the total absorption is rather arbitrary, although quite successful in previous studies of analogous nanoparticles. A different assumption or definition (for instance as the energy of the first allowed excitation) would have given different results. In addition the use of the LDA in this work, as these authors verified [5], gave much smaller energy gaps (by about 2.0 eV). In a theoretical work by Deglmann et al. [6] the structural and electronic properties, as well as ionization potentials and electronic excitation spectra of $(CdSe)_n$ clusters with sizes ranging from dimers to *n* as high as 99 were studied by *ab initio* methods. However, their calculated excitation spectra could not be directly compared to experimental measurements due to difficulties presented in the experimental preparation of small CdSe clusters in gaseous form. The polydispersity in the sizes of the experimentally prepared clusters produces featureless spectra. The use of solutions affects the surface states [6]. In another work Puzder *et al.* [7] studied $(CdSe)_n$ nanoparticles with *n* = 6, 15, 33, 45 with *ab initio* calculations. Regardless of whether the structural relaxation was performed in the presence of passivating ligands or not (gas phase), an opening in the optical gap was observed, with qualitatively (nearly quantitative) similar geometries and similar (between the two cases) midgap states. This insensitivity of the CdSe nanoclusters to passivants is referred to as a "self-healing" mechanism for the surface electronic structure (and optical gap). Different types of passivating ligands have been used in previous studies [8–13] for the passivation of the $(CdSe)_n$ clusters. One of the most commonly used is the trioctyl-phosphine oxide (TOPO). A shorter version of this molecule, trimethyl-phosphine oxide ($OPMe_3$), [11] has been also used with similar effects as TOPO. In general there is a lot of work that continues even today on the optical and electronic

properties of $(CdSe)_n$ nanoclusters, which, obviously depend on their structural properties, and the type of passivation, if any. The more recent developments about "magic" structures with non bulk-like geometry of the form of stuffed fullerenes, has given new momentum in the research of $(CdSe)_n$ clusters [3]. However, there are still conflicting results and ambiguities in the literature (especially, but not only, in earlier work) in particular with respect to the nature and size of the gap and its dependence on structure, size and composition of the nanocrystals. Obviously, an understanding and settlement of such discrepancies would be very important for further development and functionalization of $(CdSe)_n$ nanocrystals for optoelectronic applications.

In this work, in an attempt to understand and bridge the controversial results in the literature, and to uncover the general trends for $(CdSe)_n$ nanocrystals as a function of size (and structure) we have systematically and accurately (as much as possible) investigated the structural, electronic, optical, vibrational, and cohesive properties of stoichiometric $(CdSe)_n$ nanocrystals. We are using DFT calculations beyond the standard LDA, within the generalized gradient approximation (GGA), employing hybrid and non-hybrid functionals. For each n, several different initial geometries were studied, based on stoichiometric fragments cut from the bulk solid, for both zinc-blend and wurzite lattices. This is not always easy, if one tries to preserve both stoichiometry and the chosen structural pattern for a given n. We have identified, among several considered, the energetically low-lying structures for each size, n, and have studied their properties as well as the dependence of the energy gap on the various geometries. The discovery of many structures of the same size with very small energy differences (almost isoenergetic) and very large differences in energy and optical gaps, or structures with similar gaps but large energy differences can account for several discrepancies in the gap variation versus size. Obviously the

larger errors occur when many isoenergetic (or nearly isoenergetic) states (with different gaps) compete for the equilibrium geometry (ground state) structure. Comparison with experiment becomes even more problematic when various types of ligands (known or unknown) exist on the surface. The "insensitivity" of the gap to the presence of particular organic ligands on the surface is well established, and is verified here for the representative case of the n=15 nanocrystal. However, for smaller nanoparticles, the present of ligands can have strong impact on the optical gap (depending on the electronegativity of the ligands). Almost all experimental preparation techniques involve some type of ligand(s), which renders the size determination of the nanocrystals difficult, which by itself is very problematic (contrary to the optical gap measurement). This situation is very reminiscent of similar difficulties in determining the optical gap variation for silicon nanocrystals [14]. In section 2 we describe the technical details of the present calculations, including the geometry generation and optimization. The results of the present calculations are given in section 3, separately for the stoichiometric (subsection 3.1), non-stoichiometric (3.2) and ligated (3.3) nanoparticles. Finally, the conclusions of this work are summarized in section 4.

2. Theoretical and computational techniques

We have primarily studied $(CdSe)_n$ nanocrystals with n = 4, 6, 7, 8, 9, 12, 15, 20, 25, 33, and 45, based on initial "bulk-like" geometries, although we have also constructed stuffed fullerene type of structures, for n=33 and 34, in analogy to those in ref. 3 and 13, for reference purposes. In selected cases we have considered variation in stoichiometry of the form $Cd_{n\pm1}Se_n$ and $Cd_nSe_{n\pm1}$, and we have also examined (for n=8 and n=15) the influence on the geometry optimizations and on the energy and optical gaps of particular attached ligands on the surface of the nanocrystals. The calculations were performed in the framework of Density Functional Theory (DFT) and

Time Dependent Density Functional Theory. For the geometry optimization of the structures we employed the gradient corrected functional of Perdew, Burke and Ernzerhof, PBE, [15], using the def-SVP [16] basis set. The initial geometries of each set of isomers were cut from both bulk zinc blende and wurtzite crystalline structures. For each n, several different stereoisomers of the nanoparticles were constructed from both zinc blende and wurtzite crystalline structures, by performing different "cuts". These configurations were optimized with no restrictions on symmetry. For the nanoparticles with low n, around 10 different configurations for each case were studied since the possible geometries were restricted by the low numbers of atoms and the specifically chosen structural motif. However, for larger n, up to 40 different geometries were studied in each case. The low energy structures obtained from the first stage of calculations were re-optimized using the hybrid exchange-correlation functional of Becke, Lee, Yang and Parr (B3LYP) [17]. In this second round of optimizations, symmetry constraints were enforced whenever possible. It should be noted that the energy gaps calculated with PBE were 30-40% narrower than the corresponding gaps calculated with B3LYP. This could lead to conflicting results even for identical structures, studied with different functionals, although sometimes an error cancelation could occur if energy gaps (differences in Koopman's energies) are mistaken as optical gaps. For the lowest energy nanocrystals, resulting through the B3LYP optimization, vibrational analysis has been performed to determine the dynamical stability (identify vibrational modes with imaginary frequencies) and to calculate the zero point energy (ZPE) of the structures. All of our calculations were performed with the TURBOMOLE [18] suite of programs.

3. Results and Discussion

3.1 (CdSe)$_n$ nanocrystals

The lowest energy structures of the (CdSe)$_n$, n = 4, 6, 7, 8, 9, 10, 12, 15, 20, 25, 33, 45, and 60 nanocrystals obtained from initial geometries based on bulk cuts of zinc-blende and wurtzite lattices are shown in Fig. 1.
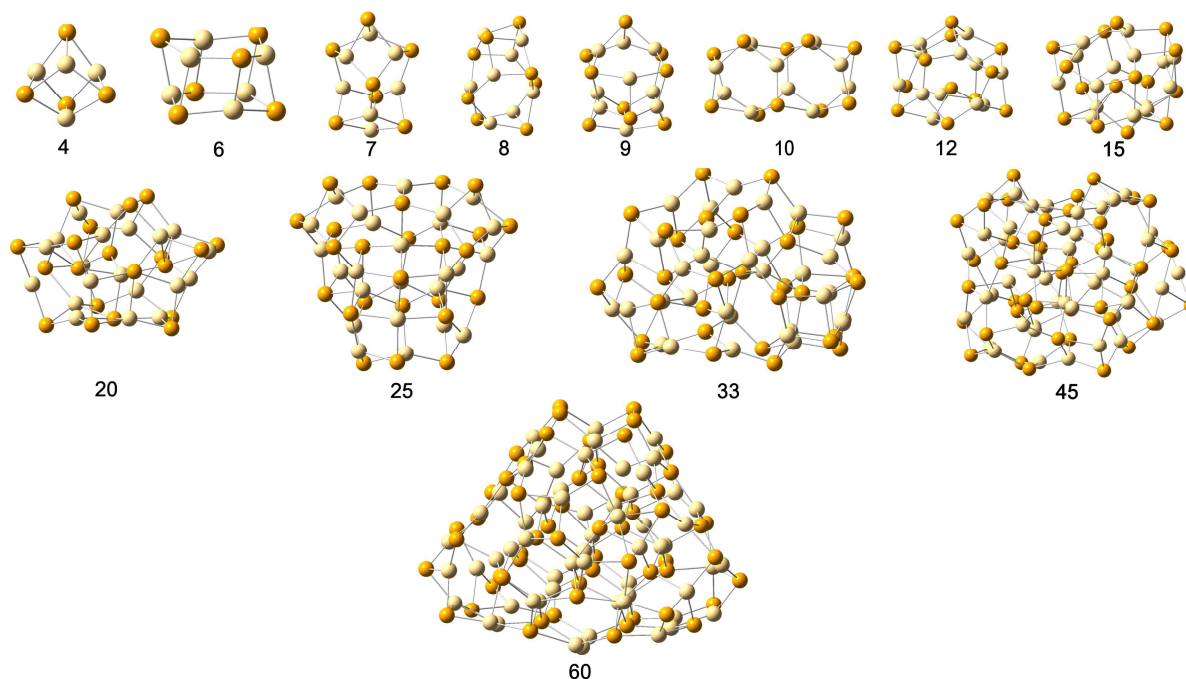

Figure 1. Lowest energy structures of (CdSe)$_n$ nanoparticles for n = 4, 6, 7, 8, 9, 10, 12, 15, 20, 25, 33, 45 and 60. Dark yellow spheres denote Se atoms. White spheres indicate Cd atoms.

For most of the nanoparticles, the lowest energy configuration resulted from a zinc-blende initial geometry with the exception of n=8, 9, and 20 that resulted from wurtzite initial geometries.

For clusters with n>15, the lowest energy geometries have no symmetry even when loose tolerance was assumed, while for all the lower n cases the structures were symmetric or near-symmetric. In particular, lowest energy nanoparticles with n=4, 5, 6, 7, 8, 9, 10, and 12 have T$_d$, D$_{3d}$, C$_{3v}$, near C$_s$, S$_4$, C$_{3h}$, C$_{2h}$, and C$_s$ symmetries, respectively. The structures of the nanoparticles, especially for n>15, follow a rather spherical structural pattern, with only a few

cases being elongated and none displaying protrusions. The average diameter is about 1nm for

the *n*=15 case and about 1.5 nm for the *n*=45 case. These results, as was mentioned earlier, do

not include fullerene type of "magic" structures of increased stability. However, in order to

access the validity of the trends and conclusions obtained in our present study, we need to

compare at some point with such "fullerene" structures, even as isolated cases. Therefore, in

analogy to the stuffed   fullerene type of magic clusters of refs. 3 and 13, we have constructed

from scratch the $(CdSe)_{33}$, and $(CdSe)_{34}$, stuffed fullerenes of Fig. 2.
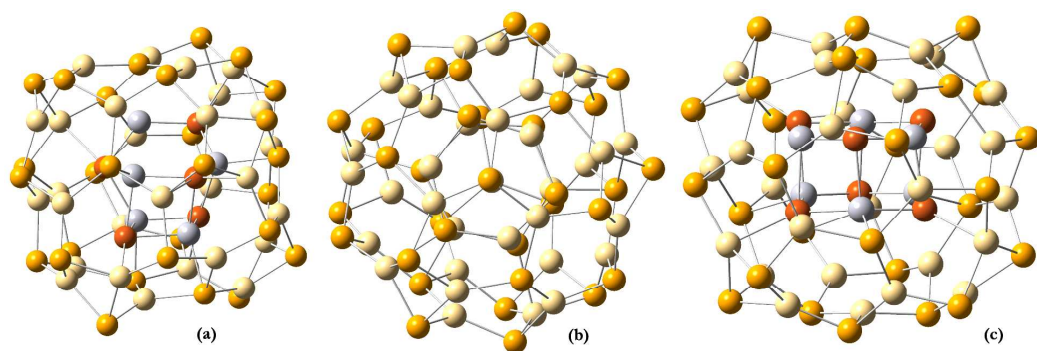
Figure 2. The (a) $(CdSe)_{33}$, and (b), (c) $(CdSe)_{34}$ cage clusters. For (a) and (c) the internal cages
have been highlighted for clarity. (b) The orientation is along the main axis of symmetry.

The stability of such clusters, which in a way are "analogous" to the "stuffed fullerene" Si_{28}

magic silicon nanoparticle, proposed by one of us [19], is expected to be much larger than the

rest in the neighborhood. The standard measure of stability of a nanoparticle is its binding

energy. The binding energy (BE) per CdSe unit is defined by the formula:

$$BE\left[(CdSe)_n\right] = \left[nE(Cd) + nE(Se) - E\left[(CdSe)_n\right]\right]/n \ , \tag{1}$$

where $E(CdSe)_n$ is the total energy of the $(CdSe)_n$ nanocrystals (with or without ZPE

correction, depending on the type of calculation), and E(Cd), and E(Se) are the atomic energies

of Cd and Se respectively (calculated at the same level of theory). The results of this calculation

are shown in Fig. 3, in which the binding energy is plotted as a function of n.
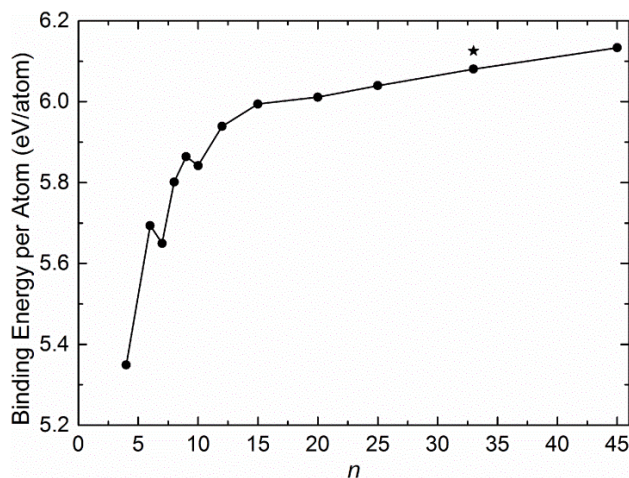
Figure 3. The binding energy vs. size (*n*) of $(CdSe)_n$ nanocrystals. The asterisk corresponds to

the magic $(CdSe)_{33}$ nanocrystal.

First of all, we can clearly verify that the n=33 cage cluster, which is not identical to any of the

literature "fullerenes", is much more stable than the corresponding bulk-based $(CdSe)_{33}$

nanocrystal, as was expected. We can also observe in Fig. 3 that the binding energy increases

with respect to the size, *n,* with the only exception the *n*=7 and 10 where a relative decrease is

noted. This could be interpreted by assuming that the n=6 and n=9 are "magic" or pseudo-

magic" numbers, with increased stability relative to their neighbors (5, 7 and 8, 10 respectively).

The magnitude of the binding energy differences for these "local" magic numbers is not of the

same size as for the "global" magic $(CdSe)_{33}$ and $(CdSe)_{34}$ nanoparticles [3,13]. Furthermore, we

can see in Fig. 3 that the binding energy of the nanocrystals rises rapidly up to about *n*=15 and

then starts slowly to saturate, reaching its maximum value at *n*=45. The binding energies,

(especially when comparing nearly isoenergetic isomers) should be always corrected for ZPE,

which sometimes could be of the same order of magnitude as the relative binding energy

between isomers. ZPE is calculated by vibrational analysis in the framework of adiabatic and harmonic approximations which lead to calculations of Infrared (IR) and (if needed) Raman spectra. At the same time frequency calculations are used to test the dynamical stability of the nanoparticles. We have performed frequency calculations for the nanoparticles with n up to 20, whereas the ZPE values for the larger clusters were estimated by linear extrapolation. No imaginary frequencies were found for any of the lowest energy final geometries of Fig. 1, which indicates that the corresponding structures are stable under vibrational distortions (they are, at least, local minima of the energy hypersurface). Table I summarizes the binding energies, zero point energies (ZPE), highest occupied molecular orbital (HOMO) – lowest unoccupied molecular orbital (LUMO) gaps (H–L gaps) and optical gaps (calculated by TDDFT) for the lowest energy structures of the $(CdSe)_n$ nanocrystals obtained in the present work.

Table I. Binding energy (ZPE corrected), HOMO–LUMO gap and optical gap for $(CdSe)_n$ nanocrystals.

n	BE_{ZPE}/atom (eV/atom)	ZPE (eV)	H-L Gap (eV)	Optical Gap (eV)
4	5.35	0.148	3.17	2.53
6	5.69	0.235	3.35	2.89
7	5.65	0.275	3.18	2.75
8	5.80	0.324	3.47	2.87
9	5.86	0.368	3.53	3.16
10	5.84	0.406	3.29	2.88
12	5.94	0.485	3.22	2.64
15	5.99	0.604	3.49	2.97
20	6.01	0.793	3.20	2.72
25	6.04	0.996[a]	3.00	2.67
33	6.08	1.314[a]	2.97	2.72
33[b]	6.13	1.314[a]	2.86	–
45	6.13	1.790[a]	2.50	–
60[c]	6.15	-	2.41	-

[a]Linearly extrapolated ZPE values.
[b]Cage structure (magic).
[c]Isolated structure without optimization

The HOMO-LUMO and optical gaps are plotted in Figs. 4(a) and 4(b) as a function of the nano particle's size. Figure 4(a) shows both HOMO-LUMO and optical gaps as a function of n. The HOMO-LUMO (and similarly the optical) gap exhibits an oscillatory behavior for n less than 15, fluctuating from a lower value of 3.17 eV for $n=4$ to a maximum value of 3.53 eV for $n=9$, but after $n=15$, it has a gradual drop reaching its lower value of 2.50 eV for $n=45$. The peaks at $n=6$ and $n=9$ are in parallel to the corresponding peaks of the binding energy in Fig.2, which we have interpreted as manifestations of some type of "magicity". This is to be expected because the HOMO–LUMO gaps are (zeroth-order) measures of kinetic stability [18] (larger gaps indicate larger chemical hardness), which however is not always in parallel with "cohesive stability measured by binding energy [18]. It is also clear from Table I that the variation of binding energy and HOMO–LUMO gaps are similar. If we keep and expand the notion that peaks in binding energy or HOMO–LUMO gaps (except for small random fluctuations) indicate "magic structures" we can conclude on the basis of our results that $n=15$ and $n=33$ should also be magic numbers for $(CdSe)_n$ nanocrystals in the context of our previous discussion. Clearly, this type of magicity, which is based on "bulk-like" nanocrystals is different from the one found for stuffed-fullerene type of structures [3, 13], although it could be indirectly related with the proposed n=13 and n=33, 34 magic numbers. The TDDFT calculated optical gaps, which by definition correspond to the energy of first allowed transition, follow the same trend as the HOMO–LUMO gaps. As we see in Fig. 4(a), the optical gaps are about 0.5 eV smaller than the HOMO–LUMO gaps. In some of the early works there was no distinction between HOMO–LUMO (Koopman's energy differences) and optical gap, which includes many-body effects. This, coupled with the ambiguity in the HOMO–LUMO gaps for different DFT functionals (PBE gaps, as was mentioned earlier, are smaller by 20–30% compared to B3LYP gaps), could give fortuitous

agreement with experimental measurements, due to error cancellation. We consider as optical gap the energy of the first allowed (with non-zero oscillator strength) excitation. However, in agreement with earlier works in the literature [10], we have found in almost all cases at least one or more excitation(s) with zero (or marginal) oscillator strengths before the first allowed transition. These excitations, which correspond to "dark transitions" [10] are considered responsible for the long radiative lifetimes observed experimentally. [10]

We can also observe, from both Table I and Fig. 4(a), that the values of HOMO–LUMO and optical gaps are larger than the bulk value of the energy gap of 1.73 eV, in contrast to the LDA HOMO-LUMO gaps, which are lower than 1eV [5a]. This is a direct result of quantum confinement and is to be expected if we consider that the largest nanocluster under study has a diameter of about 1.5 nm, well below the exciton Bohr radius for (bulk) CdSe, which is about 5.6 nm. [21]

To compare with experiment and make contact with other theoretical works, we also show the gap variation with size, in Fig. 4(b), where the "size" in this case corresponds to an average effective sphere diameter given in nanometers. Since the clusters, as we can see in Fig. 1, are not literary spherical, this is not always straightforward or unambiguous. As a result, well separated points (and graphs) of Fig. 4(a) could be in very close proximity in Fig. 4(b). This is why in Fig. 4(b) we use only points without connecting curves.

(a)

(b)
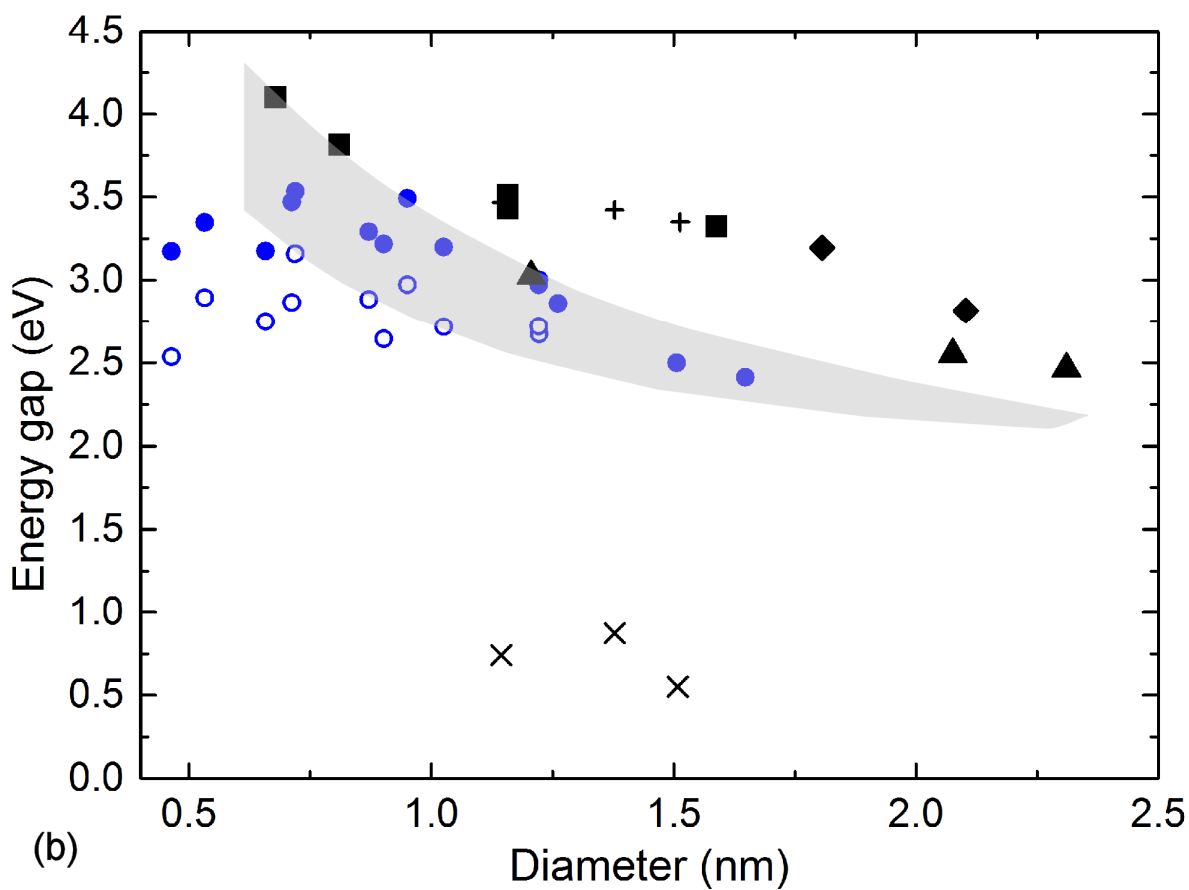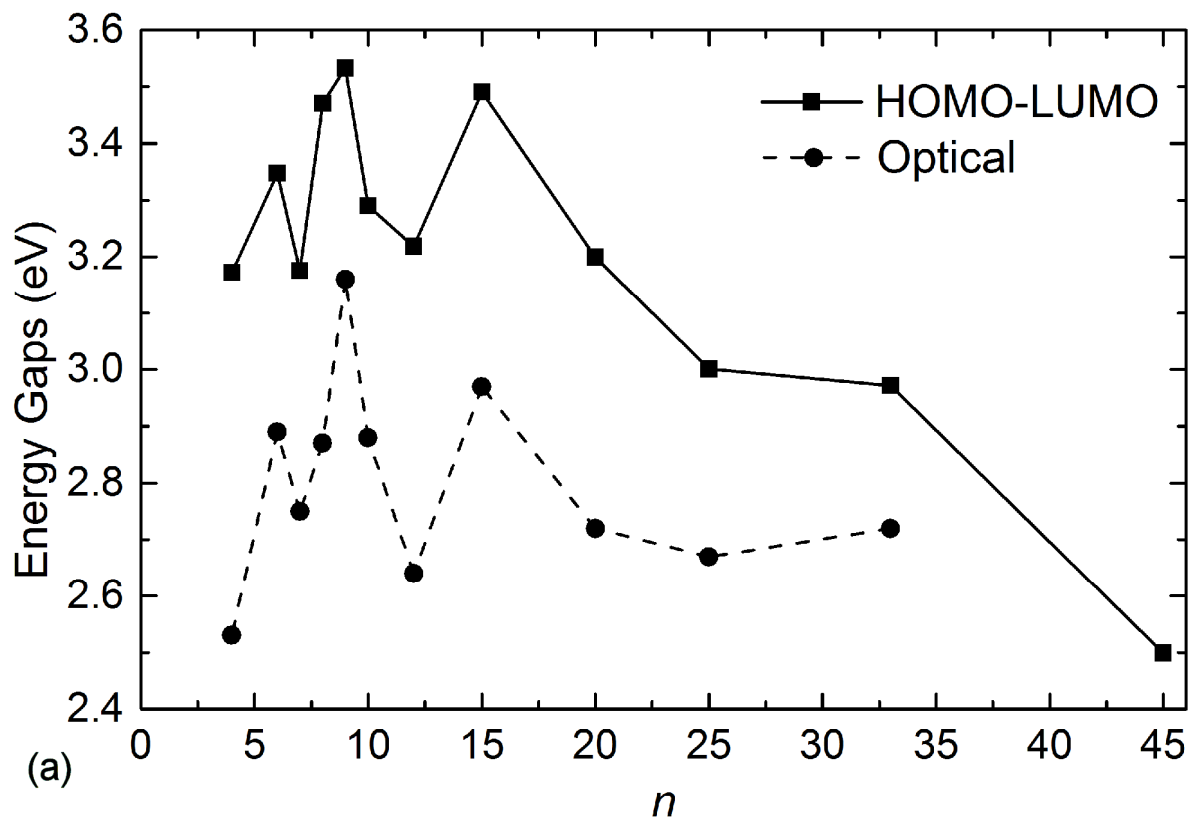
Figure 4. (a) The HOMO–LUMO (solid line) and the optical (dashed line) gap vs size, *n,* of (CdSe)$_n$ nanoparticles. (b) HOMO–LUMO and optical gaps for (CdSe) nanocrystals of various sizes. Solid and hollow blue circles correspond to theoretical values (this work). Black crosses are LDA and TDLDA theoretical values from Troparevsky *et al.* (Ref. 5a). Experimental data are shown with solid black symbols; values from Soloviev *et al.* (Ref. 22) (squares), Rogach *et al.* (Ref. 2) (diamonds) and Murray *et al.* (Ref. 23) (triangles).

Here we want to point out and emphasize the difficulties in comparisons of such data (gap versus size) between theory and experiment in one hand, and between different theoretical approaches on the other. Such difficulties are:

(a) The experimental uncertainty in determining the size of the nanoparticles, in contrast to the measurement of the gap, could be very large. The uncertainty in size is not only an experimental problem. It is very difficult (especially for the small-medium sizes) to assign an "effective" diameter for clearly non-spherical nanoparticles. The effective diameter in our study is determined by the geometrical average over three different directions. It is clear from Fig. 4(b) that slight changes (moving slightly to the left or to the right) in the "diameter" of the nanoparticles can drastically improve the agreement between theory and experiment.

(b) The existence of ligands on the surface of the nanoparticles (almost always), the exact position (and sometimes the exact composition) of which is not always clear, making extremely difficult the theoretical modeling. Although it has been clearly established that the size of the optical or HOMO-LUMO gap is insensitive to the presence of particular organic ligands, such as TOPO [8, 13] or OPMe$_3$ [11], this is not generally true for all types of ligands.

(c) The choice of the theoretical model (e.g. the choice of DFT functional or basis sets) for the ground and the excited states (e.g. the treatment of the many-body effects), and the criterion for the identification of the optical gap. It is well known that different DFT functionals can give different HOMO-LUMO gaps. It has been already pointed out that PBE gaps are about 20% - 30% smaller than B3LYP gaps for the same structure, and that LDA HOMO-LUMO gaps could be by more than 2 eV (around 100%) smaller than the corresponding TDLDA gaps [5a], as we can see in Fig. 4(b). The optical gap is normally defined as the energy of the first allowed (non zero oscillator strength) transition. Although we have applied this definition in our calculations and the results obtained (in Table I and Fig. 4), the theoretical data of Troparevsky et al. [5a] in Fig. 4(b) are calculated as the absorption threshold below which the absorption is 2% of the total absorption. Although such threshold is arbitrary, as we can see in Fig. 4(b), it seems to be very successful in comparison to the experimental data of Soloviev et al. [22]. Obviously, the adoption of such criterion of 2% would improve significantly the comparison of our results with experiment, although such "agreement" might be fortuitous. We can observe in Fig. 4(b) that our HOMO-LUMO gaps are in closer "agreement" with the experimental than the calculated optical gaps (without the criterion of 2%). The optical gap is usually calculated (as in the present work) with TDDFT or TDLDA (as in ref. 5a) using linear response theory. The hybrid functional B3LYP (as well as PBE0 [24]) has been shown to perform remarkably well in many cases even when compared to more elaborate and modern meta-hybrid and long-range corrected functionals with mean absolute errors for (non-Rydberg) excitation energies ranging from 0.18–0.34 eV [see for example Refs. 25–27]. More accurate methods based on the GW approximation combined with a solution of the Bethe–Salpeter equation, or on the quantum Monte Carlo (QMC) technique are very much time consuming even for small size systems,

although recently QMC calculations have been performed for relatively large (up to 2nm) silicon nanocrystals [28]. Surprisingly enough, these QMC calculations revealed that the static DFT/B3LYP HOMO-LUMO gaps were in better agreement with the QMC results, compared to the TTDFT/B3LYP results. This, independently of all other uncertainties discussed so far, seems to be consistent with our results in Fig. 4(b). One could possibly attribute this to lack of long-range corrections in the B3LYP functional. Long-range corrected functionals have been shown to be successful in calculating the optical gaps primarily of organic systems (oligoalchenes, organic dyes, DNA nucleobases, etc.), among others [26, 27, 29–31]. For this reason, we choose to parenthetically perform some supplementary benchmark type of calculations employing the LC-BLYP functional, which includes the long-range correction of Hirao [32]. For this purpose we use our optimized $n = 9, 15, 25$ nanocrystals, covering a significant size range with available experimental values. Although for the smallest nanocrystal $(CdSe)_9$ the agreement of the calculated optical gap of 4.22 eV with experiment is exceptional, for the larger nanocrystals $(CdSe)_{15}$ and $(CdSe)_{25}$ the calculated optical gaps (4.43 eV and 3.99 eV respectively) are overestimated compared to the experimental values, and the experimental trend is not followed (in this size-range). Furthermore, the calculated HL gaps for the $(CdSe)_n$, $n=9, 15,$ and 25 nanocrystals are overestimated: 7.88 eV, 7.98 eV, and 7.42 eV respectively. Even though the long-range corrected functional provides HL gaps of good accuracy for organic compounds [26, 27, 29–31], in the current case the calculated HL gaps are large, which may be attributed to poor treatment of the $4d$ transition metal Cd. On the other hand, the energy gaps calculated using the B3LYP functional are underestimated. However, B3LYP manages to account for the correct experimental trend throughout the size-ranges investigated here. We attribute this good behavior of B3LYP to the lack of extended charge-transfer processes.

(d) For a given theoretical model, the proper geometry optimization (relaxation) and the successful identification of the equilibrium geometry with the lowest (or near lowest) energy, among several competing isomers. In several of the early theoretical works, the structures were cut from the bulk (with or without attached ligands) and were used "as is", without proper geometry optimization and relaxation. In other instances, the chosen bulk fragments were optimized without considering other alternative isomers. Obviously, this could lead to wrong conclusions both about the binding energies (and related "magic" numbers), and the relevant energy and optical gaps. Clearly, these aspects are expected to be interrelated, similarly to the interrelation of the results in Table I. Thus, strong interrelation between the size of the binding energy and of HOMO–LUMO gaps can be seen, not only between lowest energy structures of various sizes, but also between various isomers of the same cluster [20]. As an example we have considered the $(CdSe)_n$ with $n=15$, 33, and 45 clusters. Based on the previous discussion we would expect that the lowest energy isomer would also have the largest HOMO–LUMO gap. As we can see in Table II, this is indeed the case, except perhaps for the magic $n=33$ cage cluster, which however has a completely different structural motif, and apparently different type of bonding and binding compared to the bulk generated nanocrystals. Such difference in bonding can break the analogy between cohesive and (zero[th] order) kinetic measures of stability [20]. Similarly, small "anomalies" observed for isomer # 2 for $n=15$, or isomer 4 for $n=45$, are also due to different bonding. For the isomer #2, $n=15$, this is corroborated by its structure of the HOMO and LUMO. This seems to be supported by the different overall structure of the HOMO and LUMO orbitals of this isomer, compared to the rest, as is shown below in Fig. 5.

Table II. Binding energies and HOMO–LUMO energy gaps for the lowest energy $(CdSe)_n$ isomers of the nanocrystals with $n=15$, 33, 45.

$(CdSe)_n$ Isomer	Binding Energy per atom (eV/atom)	Energy Gap (eV)
n=15		
0	6.03	3.49
1	5.88	3.15
2	5.79	1.52
3	5.76	2.07
n=33		
Magic	6.17	2.86
0	6.12	2.97
1	6.10	2.63
2	5.99	0.27
3	5.99	0.33
4	5.96	0.28
n=45		
0	6.17	2.50
1	6.17	2.16
2	6.16	1.89
3	6.16	1.25
4	6.15	2.13

It is interesting to mention that this particular nanoparticle resulted from our geometry optimization with initial geometry the (lowest energy) structure from Ref. 7. As it is very well stated in that study, the clusters self-heal by opening the gaps with the structural relaxation. On the basis of the previous discussion this is well understood, because through relaxation the structures are transformed towards the lowest energy, and therefore towards the largest gap. Obviously, the relaxation is biased by the initial geometry and the initial distribution of the valence electrons, as well as from the choice of the DFT functional. Therefore, the real, or the "global" self healing process leads to the structures of lowest energies and, consequently of the widest energy gaps.
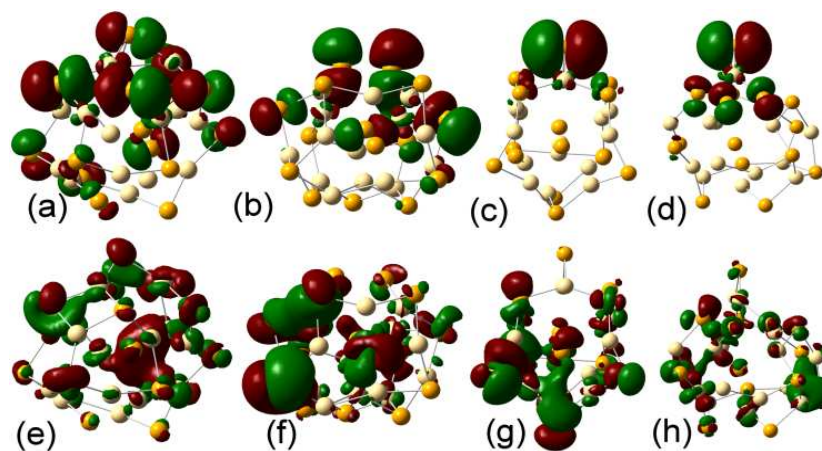
Figure 5. Molecular orbitals of the (a–d) HOMO and (e–h) LUMO states for the four lowest energy (CdSe)$_{15}$ nanoparticles. These correspond to nanoparticles $0 - 3$ of Table II. The energy of the structures increases from left to right.

Figure 5 (a–d) shows the isosurfaces (for an isovalue of 0.02) of the HOMOs for the four highest binding energy geometries shown in Table II. From the comparison between these four cases, it is apparent that for isomer with the highest binding energy the HOMO is overall delocalized on the surface, with very small contribution from the atoms (regardless of type) of the inner structure. On the surface, the HOMO is highly localized specifically over Se atoms (Se dangling bonds). This is in agreement with the findings of Puzder et al. [7]. When going successively through structures of lower energy we find that the HOMO of the low energy structures remains localized on surface Se atoms, however, the overall delocalization is significantly reduced to small regions of neighboring Se atoms (Se dangling bonds). Figure 4(e–h) shows the isosurfaces of the LUMO for the four highest binding energy cases shown in Table II. In contrast to our findings for the HOMOs, the LUMOs remain delocalized over the whole structure, i.e. inner and surfaces, and specifically over Se atoms, for all of the low energy structures of Table II. Thus for the lowest energy structure we see that HOMO and LUMO are localized in different regions in

space. This could have a profound effect in the case of attached ligands. Furthermore, this noted difference in the distribution of the HOMO between energetically different structures which however display a similar distribution pattern for the LUMO may have profound structural effects during photo(de)exitations. Excitations of the energetically higher structures result in more pronounced charge redistribution. If the deexcitation takes place adiabatically then the structure may relax to some neighboring (not only between the ones we show), energetically more favorable (but very near), configurations. Based on our finding the HOMOs of these structures are expected to be more delocalized (though always over Se atoms). A repetition of this cycle will have a similar but more diminished effect since any charge redistribution from a follow-up excitation is expected to be less significant (the HOMO of the new structure is expected to be more delocalized). This becomes more relevant if we take into account that the first permitted excitation of the energetically lowest isomer has a 92.5% HOMO to LUMO character. This mechanism may be an additional contribution to the "self-healing" mechanism of the surface electronic structure suggested by Puzder et al., [7] as well as to the relative structural insensitivity in the presence or not of ligands. [7] Obviously, the presence of any high energy barriers would terminate this mechanism. In general, the LUMO energy levels of the isomers are very close to each other. In contrast, the HOMO energies fluctuate for different geometries. This dependence of the energy gap on the structural relaxation has been attributed to the [7,11, 33–35] elimination of gap states through surface reconstruction and with the condition of the existence of up to only one dangling bond per surface atom [33,35].

For the $(CdSe)_{33}$ nanocrystal the variation of the HOMO–LUMO gaps is more abrupt. As we can see in Table II, while for the first two lowest energy structures small differences in binding energy correspond to analogous small differences in HOMO–LUMO gaps, for the next three

(CdSe)$_{33}$ isomers, differences of about 2.5% in (lower) binding energies correspond to about an order of magnitude differences in HOMO–LUMO gaps. Clearly such type of behavior i.e. structures with very small differences in stability to have such large differences in gaps, can lead to controversial and conflicting results if the calculations are performed by different groups. Similar conclusions hold true from the study of the (CdSe)$_{45}$ nanocrystal. As we can see in Table II, five different geometries have been found with very small differences in binding (less than 0.3%). As was expected, the highest binding energy structure has the widest energy gap (2.50 eV). The rest four structures, with energy differences of the order of 0.05%, have band gaps with differences up to 50%. These results emphatically support the conclusions reached from the study of the $n=33$ nanocrystal about possible sources of error in the band gaps in the literature due to many almost isoenergetic structures with very different band gaps. The general structural (and bonding) characteristics of the (CdSe)$_{33}$ and (CdSe)$_{45}$ nanocrystals, and in general of the larger ($n>15$) nanocrystals have two common features: (1) They have a near-spherical motif and (2), their surface atoms tend to satisfy at least 3 bonds with their closest neighboring atoms of other type. In contrast, geometries that are more elongated along one direction than the others or exhibit protrusions, geometries that have surface atoms with two bonds with the other type of atoms, or geometries that have neighboring surface atoms of the same type are not preferred energetically. Such structures have lower binding energies and are characterized by smaller gaps, due to the appearance of surface states inside the gap.

In order to confirm the previous statement, we have constructed (only) one (CdSe)$_{60}$ nanocrystal, cut from the bulk, which after geometry optimization ended up to a nanocrystal with binding energy of 6.01 eV/atom and HOMO–LUMO gap of 0.34 eV. Closer inspection of its geometry revealed several Cd–Cd and Se–Se bonds on its surface. By reconstructing the surface atoms in

order to eliminate those bonds and again relaxing the structure by standard geometry optimization, we ended up with a nanocrystal with a binding energy of 6.15 eV/atom (about 0.15 eV/atom higher than the previous one) and a HOMO–LUMO gap of 2.41eV. Thus, as was explained earlier, structural relaxation results in self-healing and widening of the energy gap in addition to increasing the binding energy of the nanoparticle.

3.2 $Cd_nSe_{n\pm1}$ nanoparticles

In order to examine the effect of an additional atom (or 1 atom less) in the energy gap and the overall stability, we have added one Cd or Se atom in the optimized geometries of the $(CdSe)_n$ nanoparticles with n between 6 and 9. The additional atom was placed in several different locations in the surface of the $(CdSe)_n$ nanoparticle and the corresponding structures were geometry optimized. Also, starting from the optimized $(CdSe)_{n+1}$ nanoparticles one Cd or Se atom was removed and then the structure was relaxed. The procedure was repeated for at least 10 different structures. The energy gaps corresponding to the lowest energy geometries found are shown in Table III.

Table III. The energy gaps for the lowest energy structures of Cd_nSe_m nanoparticles.

N	m	Total Binding Energy (eV)	Energy Gap (eV)
6	7	37.9756	2.87
7	6	34.6385	3.29
7	8	43.9352	1.97
8	7	40.8399	2.74
8	9	50.5212	2.90
9	8	47.1121	2.37
9	10	56.6953	3.06

10	9	53.2641	2.47

The energy gaps range from 1.97 eV for Cd_7Se_8 to 3.29 eV for Cd_7Se_6. Comparing the energy gaps in Table III with the energy gaps of the stoichiometric $(CdSe)_n$ nanoparticles in Table I, it becomes clear that the addition or removal of one Cd or Se atom results in the narrowing of the energy gap in all the cases, except in the case of Cd_6Se_7. However, this can be also seen as removal of one Cd from the corresponding Cd_7Se_7 leading to an increase in the gap, and, therefore in the overall stability due to the "magic" nature of the $n=6$ nanoparticle. Obviously, the same nanoparticle seen as an addition of one Se atom in the "magic" Cd_6Se_6 leads to lower gap (and apparently stability) by about 5%, which is the smallest narrowing of the gap. The larger change (narrowing) of the gap occurs in the case of Cd_7Se_8 nanoparticle, where there is an almost 43% narrowing of the gap. This can be probably due to a drastic change in bonding and the creation of an additional surface state, affecting largely the LUMO orbital which, as we have discussed earlier, is localized primarily on surface Se dangling bonds. As a means of estimating the relative stability of the stoichiometric nanoparticles with respect to the non-stoichiometric ones, we can calculate the change in energies and the chemical potential. By assuming that the chemical potentials μ_{Cd} and μ_{Se}, for Cd and Se respectively, for the stoichiometric and non-stoichiometric (that differ by only one Cd or Se atom) nanoparticles are the same, we can calculate the chemical potentials. The energy and binding energy differences of interest can be written in terms of the chemical potentials μ_{Cd} and μ_{Se} as:

$$\mu_{Cd} = E\left(Cd_{n+1}Se_n\right) - E\left(Cd\right) - E\left(Cd_nSe_n\right) = BE\left(Cd_nSe_n\right) - BE\left(Cd_{n+1}Se_n\right)$$

(2)

$$-\mu_{Cd} = E\left(Cd_{n-1}Se_n\right) + E\left(Cd\right) - E\left(Cd_nSe_n\right) = BE\left(Cd_nSe_n\right) - BE\left(Cd_{n-1}Se_n\right)$$

and

$$\mu_{\text{Se}} = E\left(\text{Cd}_n\,\text{Se}_{n+1}\right) - E\left(\text{Se}\right) - E\left(\text{Cd}_n\text{Se}_n\right) = BE\left(\text{Cd}_n\text{Se}_n\right) - BE\left(\text{Cd}_n\,\text{Se}_{n+1}\right)$$

$$\tag{3}$$

$$-\mu_{\text{Se}} = E\left(\text{Cd}_n\,\text{Se}_{n-1}\right) + E\left(\text{Se}\right) - E\left(\text{Cd}_n\text{Se}_n\right) = BE\left(\text{Cd}_n\text{Se}_n\right) - BE\left(\text{Cd}_n\,\text{Se}_{n-1}\right)$$

from which we get the corresponding three point approximation as:

$$2\mu_{\text{Cd}} = E\left(\text{Cd}_{n+1}\,\text{Se}_n\right) - 2E\left(\text{Cd}\right) - E\left(\text{Cd}_{n-1}\text{Se}_n\right) = BE\left(\text{Cd}_{n-1}\text{Se}_n\right) - BE\left(\text{Cd}_{n+1}\,\text{Se}_n\right)$$

$$\tag{4}$$

$$2\mu_{\text{Se}} = E\left(\text{Cd}_n\,\text{Se}_{n+1}\right) - 2E\left(\text{Se}\right) - E\left(\text{Cd}_n\text{Se}_{n-1}\right) = BE\left(\text{Cd}_n\text{Se}_{n-1}\right) - BE\left(\text{Cd}_n\,\text{Se}_{n+1}\right)$$

We apply the above equations for $n = 7$, 8, and 9 and average the three point calculated values for μ_{Cd} and μ_{Se}. The results are shown in Table IV. Our calculated average values for the chemical potentials of Cd and Se for the Cd_nSe_m nanoparticles are $\bar{\mu}_{\text{Cd}} = -1.46$ eV and $\bar{\mu}_{\text{Se}} = -4.76$ eV, respectively, with variations from the average values which are less than 9%.

Table IV. The calculated chemical potentials of Cd and Se for the Cd_nSe_m nanoparticles by three point approximation for central $(\text{CdSe})_n$ nanoparticles of size n (see eqn. (4)).

| n	μ_{Cd} (eV)	μ_{Se} (eV)
7	−1.432	−4.648
8	−1.588	−4.841
9	−1.371	−4.792
av.	−1.46	−4.76

For a given stoichiometric nanoparticle of analogous size, these values could be used to give good estimates of the binding energies of "nearby" non-stoichiometric nanoparticles.

3.3 Passivating Organic Ligands

Up to now we have described work for bare $(CdSe)_n$ "crystalline" nanoparticles, without any terminating agents (for the dangling bonds) or passivating ligands. However, in almost all experimental works, including the ones contained in Fig. 4(b), organic ligands are commonly used to stabilize the core nanocrystals [1-5]. One of the most commonly used ligand, as was mentioned earlier in the introduction, is the trioctyl-phosphine oxide (TOPO). A shorter version of this molecule, trimethyl-phosphine oxide $(OPMe_3)$, [1] has been also used with similar effects as the TOPO. In the present study, in order to examine the effect of ligands we have placed four $OPMe_3$ units at various positions around the $Cd_{15}Se_{15}$ nanocrystal for which we have considered two different lowest energy structures, isomers 0 and 1 in table II. The four $OPMe_3$ ligands were placed in different locations in the surface of the clusters with different orientations, and they were optimized. After geometry optimization for each case, we have obtained the lowest energy geometries for the two isomers. In both cases (isomers 0 and 1), the lowest energy structures were the ones in which the oxygen of the $OPMe_3$ ligands was bonded to the Cd atoms on the surface of the clusters. The energetic ordering of the structures before and after ligation was the same, i.e. the optimized cluster 0 with the additional four $OPMe_3$ still had lower energy than the optimized cluster 1 with the additional four OPMe3. This is in accord with a weak interaction energy, which is estimated to be about 0.8 eV per $OPMe_3$ unit. The HOMO-LUMO gap for the ligated cases, were 3.406 and 3.177 eV, for clusters 0 and 1, respectively. Therefore, it becomes clear that the energy (and apparently the optical) gaps are not sensitive to the presence of ligands, although the ligands are necessary for the formation and stabilization of the nanoparticles [2]. The insensitivity of the HOMO-LUMO gaps to the presence of the $(OPMe_3$ in this case) ligands can be verified from Fig. 5, which shows the frontier orbitals (HOMO–1, HOMO, LUMO) of the

lowest energy (based on isomer 0) ligated $Cd_{15}Se_{15}$ nanoparticle, together with the corresponding

orbitals of the bare (non-ligated) $Cd_{15}Se_{15}$ nanoparticle. As we can see in Fig. 5, both HOMO

and LUMO have negligible contribution from the ligands. Only the HOMO–1 orbital has a

appreciable contribution from the oxygen p orbital of one of the $OPMe_3$ units (the one in top

left). This illustrates very clearly the insensitivity of the HOMO–LUMO gap in the presence of

ligands. This insensitivity is apparently related to the relative weakness of the interaction

between the $Cd_{15}Se_{15}$ nanoparticle and the $OPMe_3$ ligands. This is in agreement with the results

of Puzder *et al*. [7].
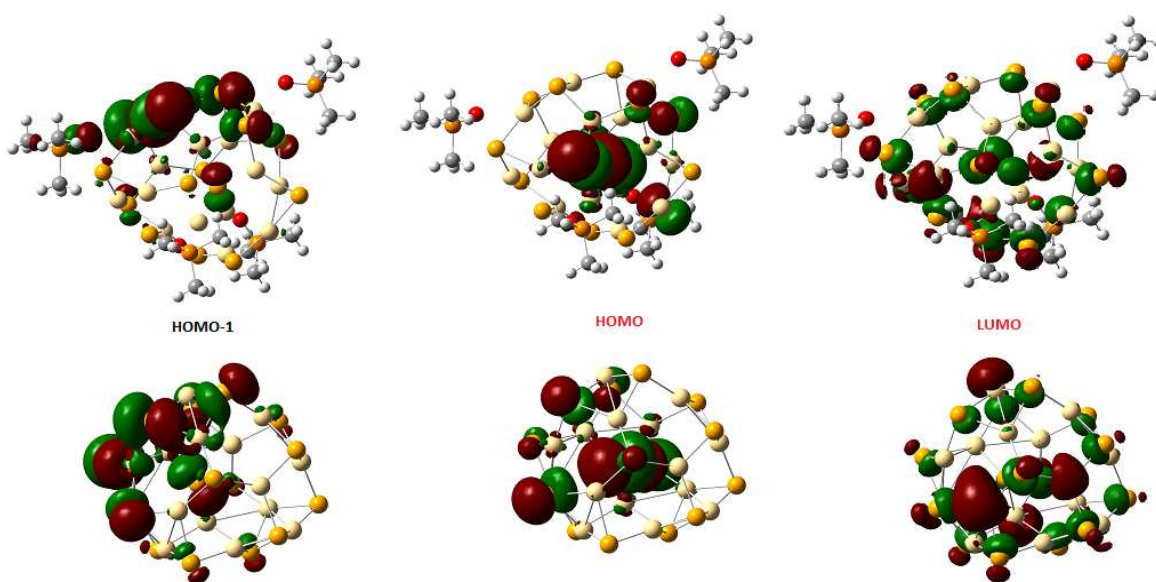
Figure 6. Molecular orbitals HOMO–1, HOMO, and LUMO states of the $(CdSe)_{15}[OPMe3]_4$
ligated nanoparticle (top), in comparison with the analogous states of the "bare" $(CdSe)_{15}$
nanoparticle

4. Conclusions

We have "generated" CdSe nanoparticles in a fully controlled and systematic way, using a large number of "cuts" (as much spherical as possible) from both zinc blende and wurtzite crystalline bulk structures, which were subsequently fully relaxed and rationalized. The relaxed structures were further examined for dynamic stability (through vibrational analysis verifying that all frequencies are real), cohesive (highest possible binding energies, from all competing structures), and kinetic stability (large HOMO–LUMO gaps), using the same ab initio theoretical approaches and techniques (all electron B3LYP/DFT and TDDFT, with SVP and TZVP basis sets) for all calculations and computations. Using this theoretical framework:

1) We have studied (and correlated) binding energies and HOMO–LUMO gaps as a function of nanoparticles' size up to $Cd_{60}Se_{60}$ (with average diameter 1.7nm). Although, our calculations reproduce the general trends and are in an overall good agreement with representative high-level calculations and particular experimental results, there are large deviations, especially for small nanoparticles, not only between our results and some other theoretical and experimental results, but also between each other (both theory and experiment). This is partly due to the difficulties in measuring the size of small nanoparticles, but mainly to the presence of passivating and stabilizing ligands.

The chosen theoretical approach could also have large impact on the results. For example, we have found, (in agreement with earlier suggestions [28]) that the calculated b3lyp HOMO-LUMO gaps could be closer to the experimental measurents, compared to the higher level TDDFT method which includes the many body effects through linear response theory. On the other hand the LDA HOMO-LUMO gaps are gross underestimations (more than 100 % off) [5a], with gaps much smaller than the infinite crystalline gap, contrary to quantum confinement. The remaining discrepancies in the literature are largely due to poor geometries, related to either non-

fully relaxed structures or failure to obtain, among several competing, the lowest energy structures.

2) We have also selectively considered non-stoichiometric nanoclusters since they are frequently used in both experiments and theory. Our calculations lead to an estimate of the atomic chemical potentials of Cd and Se, which could be used to estimate the binding energies of "nearby" non-stoichiometric nanoparticles.

3) We have examined the influence of surface passivating ligands. We have found that the relative insensitivity of the gap to the presence of particular organic ligands, such TOPO and OPMe$_3$, is related to the weakness of the interaction in conjunction to the fact that the HOMO and LUMO orbitals follow different spatial "localization".

4) The different spatial localization of the HOMO and LUMO orbitals indicates that for the manipulation and modulation of the HOMO and LUMO energy levels (band gap engineering), the spatial distribution of the ligands could be of special importance, in addition to their electronegativity.

References

1. S. Ruhle, M. Shalom, and A. Zaban, "Quantum dot sensitized solar cells'', *ChemPhysChem* **11**, 2290 (2010).

2. A.L. Rogach, A. Kornowski, M. Gao, A. Eychmüller, and H. Weller, "Synthesis and Characterization of a size series of extremely small thiol-stabilized CdSe nanocrystals", *J. Phys. Chem. B* **103**, 3065 (1999).

3. A. Kasuya, R. Sivamohan, Y.A. Barnakov, I. M. Dmitruk, T. Nirasawa, V.R. Romanyuk, V. Kumar, S.V. Mamykin, K. Tohji, B. Jeyadevan, K. Shinoda, T. Kudo, O. Terasaki, Z. Liu, R. V. Belosludov, V. Sundararajan, and Y. Kawazoe, "Ultra stable nanoparticles of CdSe revealed from mass spectrometry", *Nat. Mater.* **3** 99–102 (2004).

4. S. Pokrant, and K.B. Whaley, " Tight-binding studies of surface effects on electronic structure of CdSe nanocrystals: the role of organic ligands, surface reconstruction, and inorganic capping shells", *Eur. Phys. J. D* **6**, 255 (1999).

5. (a) M. C. Troparevsky, L. Kronik, and J. R. Chelikowsky, "Optical properties of CdSe quantum dots", *J. Chem. Phys.* **119**, 2284 (2003); (b) C. Troparevsky, and J.R. Chelikowsky, "Structural and electronic properties of CdS and CdSe clusters", *J. Chem. Phys.* **114**, 943 (2001).

6. P. Deglmann, R. Ahlrichs, and K. Tsereteli, "Theoretical studies of ligand-free cadmium selenide and related semiconductor clusters", *J. Chem. Phys.* **116**, 1585 (2002).

7. A. Puzder, A.J. Williamson, F. Gygi, and G. Galli, "Self-Healing of CdSe Nanocrystals: First-Principles Calculations", *Phys. Rev. Lett.* **92**, 217401 (2004).

8. E. Rabani, "Structure and electrostatic properties of passivated CdSe nanocrystals", *J. Chem. Phys.* **115**, 1493 (2001).

9. A. Puzder, A. Williamson, N. Zaitseva, G. Galli, L. Manna, and A. Alivisatos, "The Effect of Organic Ligand Binding on the Growth of CdSe Nanoparticles Probed by Ab Initio Calculations", *Nano Lett.* **4**, 2361–2365 (2004).

10. M. L. del Puerto, M. L. Tiago, and J. R. Chelikowsky, "Excitonic Effects and Optical Properties of Passivated CdSe Clusters", *Phys. Rev. Lett.* **97**, 096401–096404 (2006).

11. V.V. Albert, S.A. Ivanov, S. Tretiak, and S.V Kilina, "Electronic Structure of Ligated CdSe Clusters: Dependence on DFT Methodology", *J. Phys. Chem. C* **115**, 15793–15800 (2011).

12. O. Voshnyy, "Mobile Surface Traps in CdSe Nanocrystals with Carboxylic Acid Ligands", *J. Phys. Chem. C* **115**, 15927–15932 (2011).

13. M. del Ben, P.W.A. Havenith, P. Broer, M. Stener, "Density Functional Study on the Morphology and Photoabsorption of CdSe Nanoclusters", *J. Phys. Chem. C* **115**, 16782–16796 (2011).

14. (a) A. D. Zdetsis, C.S. Garoufalis and S. Grimme, "High level ab initio calculations of the optical gap of small Sillicon Quantum dots", *Phys. Rev. Lett.* **87**, 276402 (2001); (b) A. D. Zdetsis, "Optical properties of small size semiconductor nanocrystals and nanoclusters", *Rev. Adv. Mat. Sci.* **11**, 56 No 1 (2006).

15. J. P. Perdew, K. Burke, M. Ernzerhof, "Generalized Gradient Approximation Made Simple", *Phys. Rev. Lett.* **77**, 3865–3868 (1996).

16. (a) A. Schafer, H. Horn and R. Ahlrichs, "Fully optimized contracted Gaussian basis sets for atoms Li to Kr", *J. Chem. Phys.* **97**, 2571 (1992); (b) K. Eichkorn, F. Weigend, O. Treutler, and R. Ahlrichs, "Auxiliary basis sets for main row atoms and transition metals and their use to approximate Coulomb potentials", *Theor. Chem. Acc.* **97**, 119 (1997).

17. (a) A. D. Becke, "Density-functional thermochemistry. III. The role of exact exchange", *J. Chem. Phys.* **98**, 5648–5652 (1993); (b) C. Lee, W. Yang and R. G. Parr, "Development of the Colle–Salvetti correlation-energy formula into a functional of the electron density", *Phys. Rev. B* **37**, 785–89 (1988).

18. TURBOMOLE (v. 5.6), Universitat Karlsruhe, 2000.

19. A. D. Zdetsis, "One-nanometer luminous silicon nanoparticles: Possibility of a fullerene interpretation", *Phys. Rev. B* **79**, 195437 (2009).

20. A. D. Zdetsis, "Structural, Cohesive, Electronic, and Aromatic Properties of Selected Fully and Partially Hydrogenated Carbon Fullerenes", *J. Phys. Chem. C* **115**, 14507–14516 (2011).

21. (a) A. I. Ekimov, F. Hache, M. C. Schanne-Klein, D. Ricard, C. Flytzanis, I. A. Kudryavtsev, T. V. Yazeva, A. V. Rodina, and A. L. Efros, "Absorption and intensity-dependent photoluminescence measurements on CdSe quantum dots: assignment of the first electronic transitions", *J. Opt. Soc. Am. B* **10**, 100-107 (1993); (b) R.W. Meulenberg, J.R.I. Lee, A. Wolcott, J.Z. Zhang, L.J. Terminello, and T. van Buuren, "Determination of the Exciton Binding Energy in CdSe Quantum Dots", *Nano* **3**, 325–330 (2009).

22. V. N. Soloviev, A. Eichhofer, D. Fenske, and U. Banin, "Molecular Limit of a Bulk Semiconductor: Size Dependence of the "Band Gap" in CdSe Cluster Molecules" *J. Am. Chem. Soc.* **122**, 2673–2674 (2000).

23. C. B. Murray, D. J. Noms, and M. G. Bawendi, *J. Am. Chem. Soc.*, **115**, 8706-8715 (1993).

24. C. Adamo and V. Barone, "Toward reliable density functional methods without adjustable parameters: The PBE0 model," *J. Chem. Phys.* **110**, 6158–6169 (1999).

25. S. S. Leang, F. Zahariev, and M. S. Gordon, "Benchmarking the Performance of Time-Dependent Density Functional Methods" *J. Chem. Phys.* **2012**, 136, 104101.

26. D. Jacquemin, E. A. Perpète, G. E. Scuseria, I. Ciofini, and C. Adamo, "TD-DFT Performance for the Visible Absorption Spectra of Organic Dyes: Conventional versus Long-Range Hybrids", *J. Chem. Theory Comput.* **4**, 123–135 (2008).

27. A. D. Laurent and D. Jacquemin, "TD-DFT Benchmarks: A Review", *Int. J. Quant. Chem.* **113**, 2019–2039 (2013).

28. J. Williamson, J. C. Grossman, R. Q. Hood, A. Puzder, and G. Galli "Quantum Monte Carlo Calculations of Nanostructure Optical Gaps: Application to Silicon Quantum Dots" *Phys. Rev. Lett.* **89**, 196803 (2002).

29. T. Stein, H. Eisenberg, L. Kronik, and R. Baer, "Fundamental Gaps in Finite Systems from Eigenvalues of a Generalized Kohn-Sham Method", *Phys. Rev. Lett.* **105**, 266802 (2010).

30. B. M. Wong, and T. H. Hsieh, "Optoelectronic and Excitonic Properties of Oligoacenes: Substantial Improvements from Range-Separated Time-Dependent Density Functional Theory", *J. Chem. Theory Comput.* **6**, 3704–3712 (2010).

31. Michael E. Foster and Bryan M. Wong, "Nonempirically Tuned Range-Separated DFT Accurately Predicts Both Fundamental and Excitation Gaps in DNA and RNA Nucleobases", *J. Chem. Theory Comput.* **8**, 2682–2687 (2012).

32. (a) H. Iikura, T. Tsuneda, T. Yanai, and K. Hirao, "Long-range correction scheme for generalized-gradient-approximation exchange functionals," J. Chem. Phys., 115 (2001) 3540-44; (b) A. D. Becke, "Density-functional exchange-energy approximation with correct asymptotic-behavior," Phys. Rev. A, 38 (1988) 3098-100; (c) C. Lee, W. Yang,

and R. G. Parr, "Development of the Colle-Salvetti correlation-energy formula into a functional of the electron density," Phys. Rev. B, 37 (1988) 785-89.

33. S.V. Kilina, D.S. Kilin, O.V. Prezhdo, "Breaking the Phonon Bottleneck in PbSe and CdSe Quantum Dots: Time-Domain Density Functional Theory of Charge Carrier Relaxation", *ACS Nano* **3**, 93–99 (2009).

34. H. Kamisaka, S.V. Kilina, K. Yamashita, and O.V. Prezhdo, "Ab Initio Study of Temperature and Pressure Dependence of Energy and Phonon-Induced Dephasing of Electronic Excitations in CdSe and PbSe Quantum Dots", *J. Phys. Chem. C* **112**, 7800–7808 (2008).

35. M. Yu, G.W. Fernando, R. Li, F. Papadimitrakopoulos, N. Shi, R. Ramprasad, "First Principles Study of CdSe Quantum Dots: Stability, Surface Unsaturations, and Experimental Validation", *Appl. Phys. Lett.* **88**, 231910-1–3 (2006).

TOC image, 8cm x 4cm.
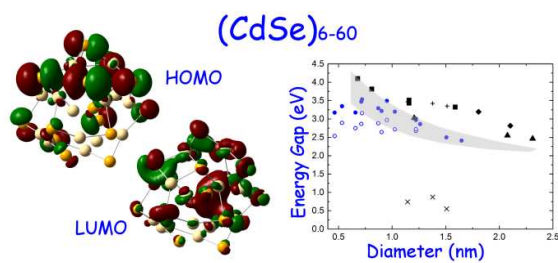
HOMO–LUMO and optical gaps of $(CdSe)_n$ nanocrystals appear to have controversial magnitudes and size dependence, which we have rationalized.